Nanoscale Res Lett (2009) 4:1447–1451
DOI 10.1007/s11671-009-9418-3

NANO EXPRESS

# The Influence of an Adsorbate Layer on Adatom Diffusion and Island Nucleation: Fe on Si(111)-$\sqrt{3} \times \sqrt{3}$-Au

**K. Paredis · D. Smeets · A. Vantomme**

Received: 5 June 2009 / Accepted: 12 August 2009 / Published online: 26 August 2009


**Abstract** Using scanning tunneling microscopy, the influence of a thin Au layer on the diffusion of Fe adatoms and the subsequent island nucleation on a Si(111) surface is investigated. The adsorbate induces the Si(111)-$\sqrt{3}\times\sqrt{3}$-Au structure that increases the surface mobility of subsequently deposited Fe atoms, resulting in the formation well-defined nanoclusters. Surprisingly, the domain walls—inherent to the $\sqrt{3} \times \sqrt{3}$-Au reconstruction—do not influence the surface diffusion, which demonstrates that the passivation is of much more importance for the self-assembly than the surface corrugation. Using the decoupling of the diffusion and nucleation *on* the surface and the reaction *with* the surface and conventional nucleation theory, the activation energy for surface diffusion $E_d = 0.61$ eV and the critical cluster size $i = 3$ are determined, which reveal the microscopic details of the diffusion and nucleation processes.

**Keywords** Self-assembly · Surface reconstruction · Diffusion · Passivation · STM · Nanostructures · Iron silicide

## Introduction

In order to assure the continuing downscaling of electronic components, new growth methods need to be explored as currently used top-down techniques are approaching their physical limits. An emerging alternative for the growth of nanoscale systems is self-assembly: by exploiting the striving toward the minimal energy it enables the formation of nanostructures even down to the atomic level. However, its future implementation requires extensive fundamental research to unravel the complex interactions involved. Self-assembly of nanostructures on a surface is predominantly governed by two physical processes: the diffusion of atoms and the subsequent island nucleation. The combination of these processes eventually determines the final properties of the nanostructured systems, such as size, distribution, phase, electrical and magnetic properties, etc. Considering the key role of the surface in the implied interactions, surface functionalization provides a potential way to influence—and eventually to control—the growth of nanostructures on a surface. Our recent results on noble metal induced surface reconstructions prove that an ultra thin buffer layer and the induced surface structure have a major influence on the final morphological island properties [1–3]. In order to obtain a better understanding of the microscopic details of the self-assembly process, we investigated in detail the effect of the Au-induced Si(111)-$\sqrt{3} \times \sqrt{3}$-Au superstructure on the subsequent diffusion of adatoms and the nucleation of Fe-Si nanostructures on Si(111). Whereas we previously investigated the morphological properties (e.g., size, height, phase formation, density, etc.) of the islands on different Au-induced surface reconstructions [3] and the Cu-induced reconstruction [2], we now specifically focus on the Si(111)-$\sqrt{3} \times \sqrt{3}$-Au reconstruction to investigate the microscopic details of the diffusion and nucleation processes on this particular surface. As it consists of $\sqrt{3} \times \sqrt{3}$ domains separated by domain walls that may act as non-reactive diffusion barriers, a study of the influence of these domain walls on subsequent nanostructure formation can reveal the relative importance of the surface topography versus the surface passivation. Furthermore, to determine

K. Paredis (✉) · D. Smeets · A. Vantomme
Instituut voor Kern- en Stralingsfysica and INPAC, K. U. Leuven, Celestijnenlaan 200D, 3001 Leuven, Belgium
e-mail: kristof.paredis@fys.kuleuven.be

the relevant kinetic parameters for surface diffusion and island nucleation on the Si(111)-$\sqrt{3} \times \sqrt{3}$-Au superstructure, the results are interpreted in the framework of the conventional nucleation theory. It is elaborated that this theory is applicable for our system and as such, we present a novel approach for interpreting surface diffusion and island nucleation in reactive systems.

## Experimental

In analogy to our previous work [3], Si(111) samples (FZ, 8–12 Ω cm) were cleaned ex situ in a 2% HF solution and in situ using a two-step silicon-flux method [4]. This procedure results in a clean Si(111) surface that exhibits the well known Si(111)-7 × 7 reconstruction. Subsequent deposition of 0.76–0.96 ML Au (1 ML = $7.83 \times 10^{14}$ at/cm$^2$) at room temperature followed by a 30 min. annealing at 700°C results in the formation of the Si(111)- $\sqrt{3} \times \sqrt{3}$-Au reconstruction which is thermally stable up to 700°C and exhibits no dangling bonds [5]. A conventional molecular-beam epitaxy (MBE) set-up with a base pressure of $5 \times 10^{-11}$ Torr was used to deposit the Si, Au and Fe. The deposition rate was monitored in situ with a quartz crystal microbalance, which was calibrated using Rutherford backscattering spectrometry and X-ray reflectivity and was kept constant at 0.015 ML/s for all Fe depositions. After deposition, the sample cooled down and was investigated at room temperature in vacuo by scanning tunneling microscopy (STM). All substrates used in this work have an unintentional miscut of approximately 0.6° relative to the [111] direction and consequently exhibit surface steps. Due to step bunching, the terraces have widths ranging from 30 to 150 nm.

## Results and Discussion

To demonstrate the effect of the $\sqrt{3} \times \sqrt{3}$ reconstruction on the self-assembly of nanostructures [3], we have first deposited 0.28 ML Fe at 300°C on the bare Si(111)- 7 × 7 surface as a reference. The resulting surface morphology is presented in Fig. 1a. A closer look at the surface reveals a high density of very small grains, randomly distributed. This growth behavior finds its origin in the high concentration of dangling bonds present on the 7 × 7 surface. As a consequence, the surface is highly reactive, thus strongly limiting the diffusion of deposited Fe atoms on the surface: the Fe atoms will rapidly react with the Si surface atoms upon arrival. Next, deposition of the same amount of Fe onto the Si(111)-$\sqrt{3} \times \sqrt{3}$-Au superstructure at 300°C results in the formation of well-defined nanostructures, as presented in Fig. 1b. Meanwhile, the $\sqrt{3} \times \sqrt{3}$ structure

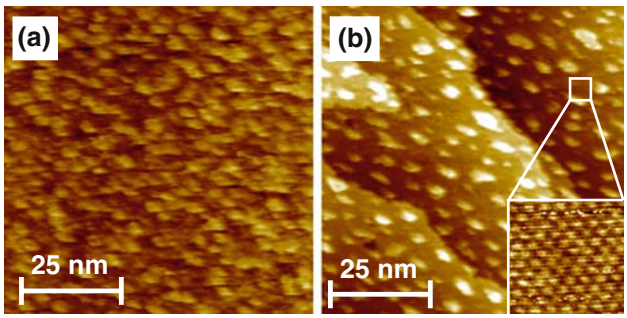


**Fig. 1** STM micrographs of the surface morphology after deposition of 1.1 ML Fe at 300°C onto (**a**) the bare Si(111)-7 × 7 surface and (**b**) the Si(111)-$\sqrt{3} \times \sqrt{3}$-Au surface. (inset) Atomic resolution image of the Si(111)-$\sqrt{3} \times \sqrt{3}$-Au structure

remains present on the entire surface, as evidenced by the inset of Fig. 1b. The drastic change in growth kinetics is induced by the Si(111)-$\sqrt{3} \times \sqrt{3}$-Au surface, which exhibits no dangling bonds and therefore, is by far less reactive than the 7 × 7 structure. This lower reactivity delays the reaction with the Si atoms and causes a strong increase in the Fe surface diffusion, resulting in the formation of distinct nanoclusters, as discussed previously [3]. We want to emphasize that, as a result of the Au passivation, we are able to create a silicon surface with a strongly reduced reactivity, which is essential for the correct interpretation of our results below.

As mentioned in the introduction, the Si(111)-$\sqrt{3} \times \sqrt{3}$-Au surface structure exhibits a large density of domain walls separating the $\sqrt{3} \times \sqrt{3}$ domains on the surface (see Fig. 2a). They contain the excess Au atoms residing on top of the $\sqrt{3} \times \sqrt{3}$ reconstruction which explains the critical dependence of their density on the deposited Au coverage [6]. Therefore, these walls are also referred to as "heavy" walls. The influence of the extra surface corrugation induced by these domain walls on the surface diffusion of Fe atoms, is investigated by depositing 0.28 ML Fe at 400°C onto surfaces with a varying domain wall density. For instance, in Fig. 2b, the surface morphology after deposition onto the surface shown in Fig. 2a is presented. The density is quantified by the number of domain wall intersections with an artificial, regular grid, divided by the total length of the grid (yielding a domain wall density in nm$^{-1}$), as demonstrated in the lower right corner of Fig. 2a. The results are presented in Fig. 2c, where the island density after Fe deposition is plotted as a function of the domain wall density on the surface prior to deposition. These results surprisingly show that, within the investigated range and the experimental uncertainty, there is no influence of these domain walls on the island density. As the island density is inversely related to the characteristic diffusion length, i.e. the average distance between two neighboring islands, it is evidenced that the diffusion

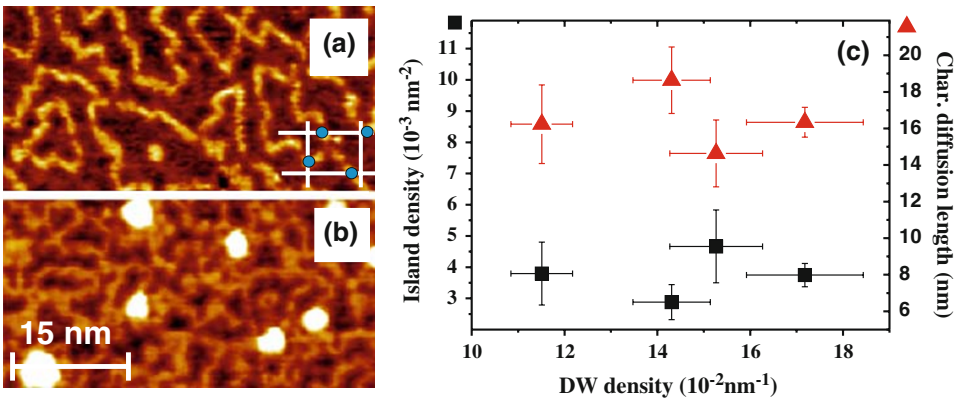


**Fig. 2** **a** The Si(111)-$\sqrt{3} \times \sqrt{3}$-Au surface structure, characterized by a high density of domain walls. In the lower right corner, the grid used for determining the DW density is indicated, together with the intersections. **b** The surface in (**a**) after deposition of 1.1 ML Fe at 400°C showing a strong increase in domain wall density. **c** Island density (*squares*) after Fe deposition and characteristic diffusion length (*triangles*) as a function of the initial domain wall (DW) density prior to Fe deposition

length ($\sim$17 nm), despite being significantly larger than the typical distance between the domain walls (5–9 nm), does not decrease with increasing domain wall density (see Fig. 2c). Consequently, the presence of these domain walls does not alter the surface potential as felt by the Fe atoms. This is schematically shown in Fig. 3, where the typical surface topography of the Si(111)-$\sqrt{3} \times \sqrt{3}$-Au surface (a) is represented together with a suggested representation of the surface potential (b). Because the domain walls do not have a significant influence on the surface potential, they are invisible in the potential landscape. These results seem to be in contradiction with previous observations of Nagao et al. who claim that surface diffusion of Mn atoms is severely hindered by the surface corrugation induced by the domain walls [7]. Nagao et al. draw these conclusions based on the comparison of Mn diffusion on *different* surface reconstructions (Si(111)-$\sqrt{3} \times \sqrt{3}$-Ag, Si(111)-$\sqrt{3} \times \sqrt{3}$-Au and Si(111)-6 × 6-Au), but they do not provide evidence on the question of whether the diffusion is limited by the domain walls or, on the other hand, by the specific reconstruction itself. However, we have performed a comparative study on a *single* reconstruction, specifically investigating the role of the domain walls. Nevertheless, the result is quite unexpected as one would intuitively assume that domain walls influence surface diffusion, based on a comparison of different reconstructions [3]. Atomic steps on the other hand, do show up in the representation of the surface potential (see discussion below). This conclusion points out that the chemical passivation of the Si dangling bonds is of much greater importance for the subsequent diffusion than the surface corrugation induced by the domain walls. This result is of major importance for the general understanding of surface diffusion.

On the other hand, the STM observations in Fig. 2 reveal that island nucleation itself has a large impact on the domain wall density. In Fig. 2a a $\sqrt{3} \times \sqrt{3}$ surface is shown prior to Fe deposition with an average domain wall density of $14 \pm 1 \times 10^{-2}$nm$^{-1}$ while after Fe deposition (0.28 ML at 400°C), the average density has significantly increased to $33 \pm 2 \times 10^{-2}$nm$^{-1}$ (Fig. 2b). As the domain wall density is directly correlated to the Au coverage on the surface, we can conjecture that the Fe atoms penetrate into the Au layer after nucleation, thereby expelling the Au atoms. These atoms are redistributed over the remaining

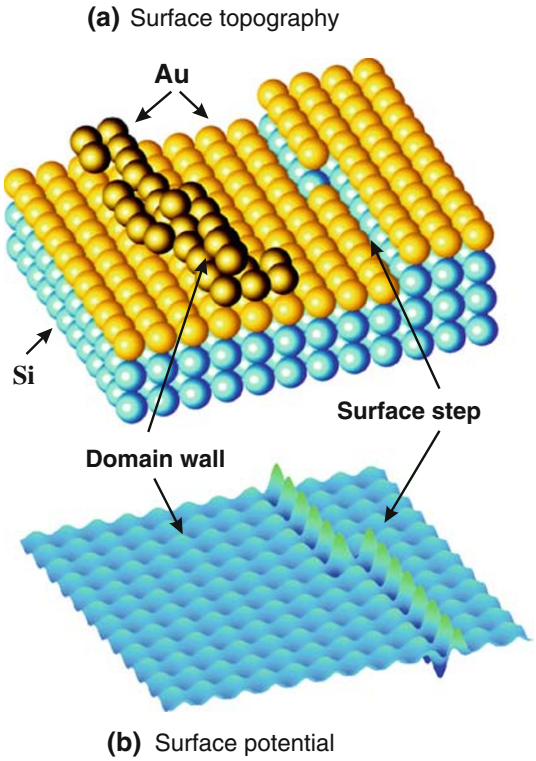


**Fig. 3** Schematic representation of the typical surface topography of the Si(111)-$\sqrt{3} \times \sqrt{3}$-Au surface (**a**) with a suggested representation of the corresponding surface potential (**b**)

Si(111)-$\sqrt{3} \times \sqrt{3}$-Au surface which results in the creation of new domain walls, as previously shown in [3]. In the same reference, we have discussed that the islands consist of an iron silicide as well. Consequently, the Au layer acts as a surfactant which significantly enhances the diffusion, but does not inhibit the reaction between the nucleated Fe nanoclusters and the Si substrate. This reaction between the Fe adatoms and the Si substrate is driven by the large difference in the heat of formation ($\Delta H$ = $-39.56$ kJ mol$^{-1}$ for Fe–Si compared to $-17.5$ kJ mol$^{-1}$ for Au–Si) [8–10]. We want to stress that based on these observations, the Au layer causes a decoupling of the diffusion and nucleation *on* the surface and the reaction *with* the surface as Fe diffusion and island nucleation take place before the reaction with the substrate occurs. Naturally, the preservation of the reaction is of major importance for the future growth of *binary* nanostructures.

As it turns out that the domain wall density does not have a major influence on the island formation on Si(111)-$\sqrt{3} \times \sqrt{3}$-Au, different Au coverages on Si(111) will result in the same island formation which opens a process window for surface functionalization. This encouraged us to further investigate the island formation on this particular surface. We therefore deposited 0.28 ML of Fe onto the Si(111)-$\sqrt{3} \times \sqrt{3}$-Au surface at temperatures ranging from 300 to 600°C to study the cluster growth kinetics. The STM micrographs in Fig. 4 show the surface morphology after deposition at 300°C (a), 400°C (b) and 600°C (c). As the temperature increases, a significant increase in island size is observed. The size distributions in Fig. 5a quantitatively show the increase in mean island size from 1.93 ± 0.10 nm$^2$ at 300°C to 666 ± 20 nm$^2$ at 600°C. Moreover, the island height increases considerably with increasing temperature (from 0.23 ± 0.01 nm to 7.11 ± 0.10 nm) as well, as is evidenced by the height distributions in Fig. 5b (the height is measured relative to the terrace). Both observations are explained by the increase in diffusion length caused by the elevated temperatures.

Additionally, it is observed that the islands preferentially form at the lower step edge at 600°C, (see Fig. 4c), whereas at 300 and 400°C the dots randomly nucleate on the terraces and the step edges (see Fig. 4a, b). This phenomenon is the result of both the passivating Au layer and the elevated temperature, which allow the Fe atoms to reach the step edges, as typical diffusion lengths at 600°C are of the order of 110 nm, which is considerably larger than the average terrace width observed on this surface (approx. 66 nm). These highly coordinated sites are energetically favorable due to the easy access to Si atoms. This is also represented in the schematic diagram in Fig. 3: a surface step gives rise to a local minimum in the surface potential which traps diffusing Fe atoms. Consequently, the Au interlayer not only allows to control diffusion (i.e. island density and size), but also allows to alter the preferential nucleation site.

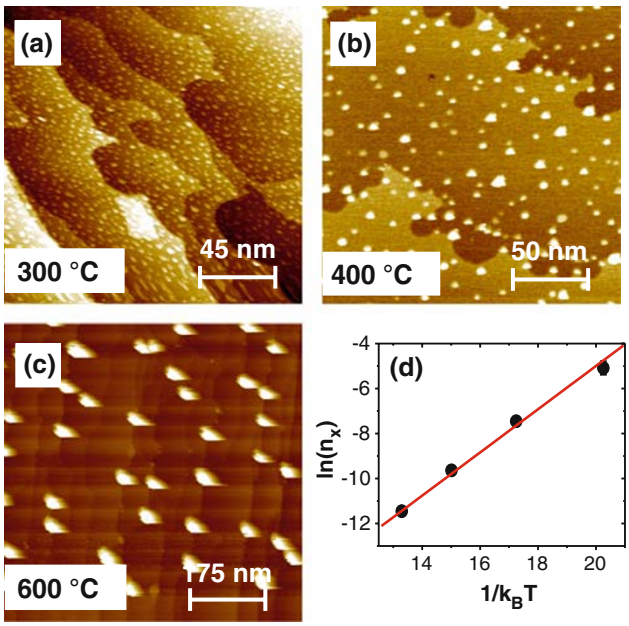


**Fig. 4** STM images of the surface morphology after deposition of 0.28 ML Fe at **a** 300°C **b** 400 °C and **c** 600°C onto the Si(111)-$\sqrt{3} \times \sqrt{3}$-Au surface. **d** Arrhenius plot of the island density, along with a fit to the data according to the conventional nucleation theory

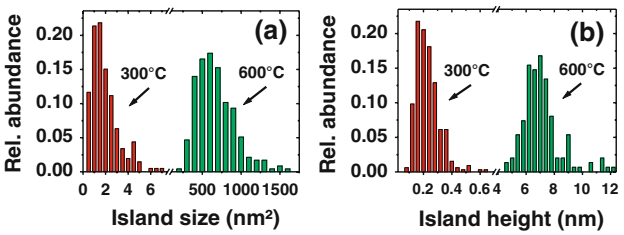


**Fig. 5** **a** Island size distribution and **b** island height distribution after deposition of 0.28 ML Fe at 300 and 600 °C on the Si(111)-$\sqrt{3} \times \sqrt{3}$-Au surface. Note the different scale of the *x*-axis for both temperatures

As the diffusion length increases, the island density decreases as well (see Fig. 4a–c). This behavior is predicted by the conventional nucleation theory, which essentially describes the formation kinetics of nanoclusters on a surface [11, 12]. Originally, the theory was developed for non-reactive systems. However, our new approach to apply this theory to reactive systems is justified as the surface largely resembles an inert surface from diffusion point of view, due to the decoupling of the diffusion and nucleation on the one hand, and the reaction processes on the other hand. While diffusing over the surface, the Fe adatoms might encounter each other and form a nucleus. Whether the nucleus is stable or decays to a smaller cluster is determined by its size. Within the conventional

nucleation theory the threshold is defined by the concept of the critical nucleus size $i$ defining the largest unstable cluster which will, upon addition of one extra atom, render stable. Furthermore, according to this theory, the density of stable islands $n_x$ decreases exponentially with increasing temperature:

$$n_x = \eta \left(\frac{F}{D_0}\right)^{(i/i+2)} \exp\left(\frac{E^*}{kT}\right). \quad (1)$$

In this equation $\eta$ represents a constant dimensionless number near 0.2 containing the coverage dependence, $F$ is the deposition flux, $D_0$ is the surface diffusion prefactor, $i$ is the critical nucleus size, and $E^* = (iE_d + E_b)/(i + 2)$ is the effective diffusion barrier, which is a weighted sum of the activation energy for diffusion $E_d$ and the critical cluster binding energy $E_b$. The energy parameter $E^*$ is experimentally accessible from the slope of $\ln(n_x)$ vs. $1/kT$, whereas the critical nucleus size can be obtained from the $1/T = 0$ intercept. In Fig. 4d, the Arrhenius plot of the island density $n_x$ is shown together with a fit to the data yielding the energy parameter $E^* = 0.96 \pm 0.05$ eV and the critical nucleus size $i = 3.1 \pm 0.3$ (using the known flux 0.015 ML/s and nominal values $D_0 = 10^{14}/s$ and $\eta = 0.2$) [11, 12]. This implies that a cluster of four atoms is stable and defines a nanostructure. With the value $i = 3$, the expression for the effective diffusion barrier becomes $E_d + \frac{1}{3}E_3 = \frac{5}{3}E^* = 1.60 \pm 0.10$ eV, with $E_3$ the binding energy of a three-atom cluster. In order to calculate the activation energy $E_d$, the binding energy of a free $Fe_3$ cluster is used as an estimate for $E_3$, since the Au-passivated surface can be considered inert. Taking the value $E_3 = 2.96 \pm 0.20$ eV, reported by Lian et al. [13], we find an activation energy for Fe diffusion on the Si(111)-$\sqrt{3} \times \sqrt{3}$-Au surface of $E_d = 0.61 \pm 0.12$ eV, which is lower than the value published by Wohllebe et al. [14] for Fe diffusion on a Si(111)-7 × 7 surface, $E_d = 0.76 \pm 0.10$ eV, in accordance with our observations and expectations. However, it is important to point out here, to be very careful with the comparison with these literature data since they are determined using a theory developed for a non-reactive surface in a study of a (highly) reactive Si surface. For a fully quantitative comparison, reliable values for Fe diffusion on Si(111)-7 × 7, that are currently unavailable, are essential. Nevertheless, the values for the activation energy of the surface diffusion $E_d$ and the critical nucleus size $i$ are particularly important for the Si(111)-$\sqrt{3} \times \sqrt{3}$-Au surface since they determine the microscopic diffusion and nucleation mechanisms on the passivated surface and allow to predict the island density, size and height for a given temperature and deposition rate, which is a key feature in the controlled growth of nanostructures.

## Conclusions

In conclusion, we have shown that an ultrathin Au layer has a drastic influence on the subsequent growth of Fe-based nanostructures on the Si(111) surface. Surprisingly, the surface corrugation induced by the domain walls, inherent to the $\sqrt{3} \times \sqrt{3}$-Au reconstruction, does not significantly affect the surface diffusion. This demonstrates that the passivation of the surface plays a much larger role in the adatom diffusion than the surface topography, which is of major importance for the understanding of surface diffusion. Using a novel approach by applying conventional nucleation theory to this reactive system, we determined the activation energy for surface diffusion on Si(111)-$\sqrt{3} \times \sqrt{3}$-Au, $E_d = 0.61$ eV and the critical nucleus size $i = 3$, exposing the microscopic details of the diffusion and nucleation mechanisms. Moreover, these parameters allow to predict the island density, the island size and the island height for a given deposition temperature and rate, which is a major prerequisite in controlling nanostructure growth.

**Acknowledgments** This work was supported by the Fund for Scientific Research, Flanders (FWO), the Concerted Action of the KU-Leuven (GOA/2009/006), the Interuniversity Attraction Pole (IAP P6/42) and the Center of Excellence Programme (INPAC EF/05/005).

## References

1. K. Vanormelingen, K. Paredis, A. Vantomme, J. Appl. Phys. **98**, 024302 (2005)
2. K. Paredis, K. Vanormelingen, A. Vantomme, Appl. Phys. Lett. **92**, 043111 (2008)
3. K. Paredis, D. Smeets, A. Vantomme, Nanotechnology **20**, 075607 (2009)
4. M. Herman, H. Sitter, *Molecular Beam Epitaxy, Springer Series in Materials Science*, vol 7. (Springer, Berlin, 1989)
5. G. Le Lay, Surf. Sci. **132**, 169 (1983)
6. T. Nagao, S. Hasegawa, K. Tsuchie, S. Ino, C. Voges, G. Klos, H. Pfnur, M. Henzler, Phys. Rev. B **57**, 10100 (1998)
7. T. Nagao, S. Ohuchi, Y. Matsuoka, S. Hasegawa, Surf. Sci. **419**, 134 (1999)
8. E. Moroni, W. Wolf, J. Hafner, R. Podloucky, Phys. Rev. B **59**, 12860 (1999)
9. A. Miedema, R. Boom, F. De Boer, J. Less Common Met. **41**, 283 (1975)
10. A. Miedema, J. Less Common Met. **46**, 67 (1976)
11. J.A. Venables, G.D.T. Spiller, M. Hanbücken, Rep. Prog. Phys. **47**, 399 (1984)
12. H. Brune, Surf. Sci. Rep. **31**, 121 (1998)
13. L. Lian, C.-X. Su, P. Armentrout, J. Chem. Phys. **97**, 4072 (1992)
14. A. Wohllebe, B. Holländer, S. Mesters, C. Dieker, G. Crecelius, W. Michelsen, S. Mantl, Thin solid films **287**, 93 (1996)